Supplementary Material

Sedimentation and Transport of Different Soil Colloids: Effects of Goethite and Humic Acid

Yali Chen [1,2], Jie Ma [1,2,*], Xiaojuan Wu [2], Liping Weng [1,2,3,*] and Yongtao Li [2,4]

[1] Key Laboratory for Environmental Factors Control of Agro-Product Quality Safety, Ministry of Agriculture and Rural Affairs, Tianjin 300191, China; chenyali@caas.cn (Y.C.); wengliping@caas.cn (L.W.)

[2] Agro-Environmental Protection Institute, Ministry of Agriculture and Rural Affairs, Tianjin 300191, China; 18518941166@163.com (X.W.); yongtao@scau.edu.cn (Y.L.)

[3] Department of Soil Quality, Wageningen University, P.O. Box 47, 6700, AA, Wageningen, The Netherlands

[4] College of Natural Resources and Environment, South China Agricultural University, Guangzhou 510642, China

* Correspondence: majie@caas.cn (J.M.); wnegliping@caas.cn (L.W.)

List of contents

S1. Colloid transport models

The convection diffusion equation (CDE) with two kinetic retention sites was employed to describe the colloid transport and retention in the column experiments as Equation (1) [1, 2].

$$\frac{\partial C}{\partial t} = -\frac{v}{\theta}\frac{\partial C}{\partial z} + D\frac{\partial^2 C}{\partial z^2} - \frac{\rho}{\theta}\frac{\partial s_1}{\partial t} - \frac{\rho}{\theta}\frac{\partial s_2}{\partial t} \quad (1)$$

θ ($cm^3 \cdot cm^{-3}$) is the volumetric water content; D is the dispersion coefficient ($m^2 \cdot s^{-1}$); ϱ ($g \cdot m^{-3}$) is the column dry bulk density; z (cm) is the spatial coordinate; ν ($cm \cdot min^{-1}$) is the Darcy's velocity; and s_1 ($g \cdot g^{-1}$) and s_2 ($g \cdot g^{-1}$) are colloid concentrations deposited in Site-1 and Site-2, respectively.

The Site-1, first kinetic site, on which the retention of colloid is assumed to be reversible, whereas Site-2, the second kinetic site, on which the retention is assumed to be irreversible, time-dependent retention, as described by the Langmuirian blocking or depth-dependent retention. s_1 on Site-1 and s_2 on Site-2 are given in Equations (2) and (3), respectively.

$$\frac{\rho}{\theta}\frac{\partial s_1}{\partial t} = k_{1a}C - \frac{\rho}{\theta}k_{1d}s_1 \quad (2)$$

$$\frac{\rho}{\theta}\frac{\partial s_2}{\partial t} = \psi_t k_{2a} C \quad (3)$$

k_{1a} (min^{-1}) and k_{2a} (min^{-1}) are first-order retention coefficients on Site-1 and Site-2, respectively; k_{1d} (min^{-1}) is the first-order detachment coefficient; ψ_t (dimensionless) is parameters to account for time-dependent retention. The Langmuirian blocking function and the depth-dependent retention function define ψ_t are expressed by Equations (4) and (5), respectively.

$$\psi_t = 1 - \frac{s_2}{s_{max2}} \quad (4)$$

$$\psi_t = \left(\frac{d_c - x}{d_c}\right)^{-\beta} \quad (5)$$

s_{max2} ($g \cdot g^{-1}$) is the maximum colloid concentration on Site-2; d_c is the median diameter of the sand grains (cm); and β (dimensionless) is an empirical variable that controls the shape of the retention profile, using an optimal value of 0.432 for different sized spherical colloid and sand grains in which significant depth-dependency (hyperexponential retention profiles) occurred [1].

S2. XRD analysis of soil colloids

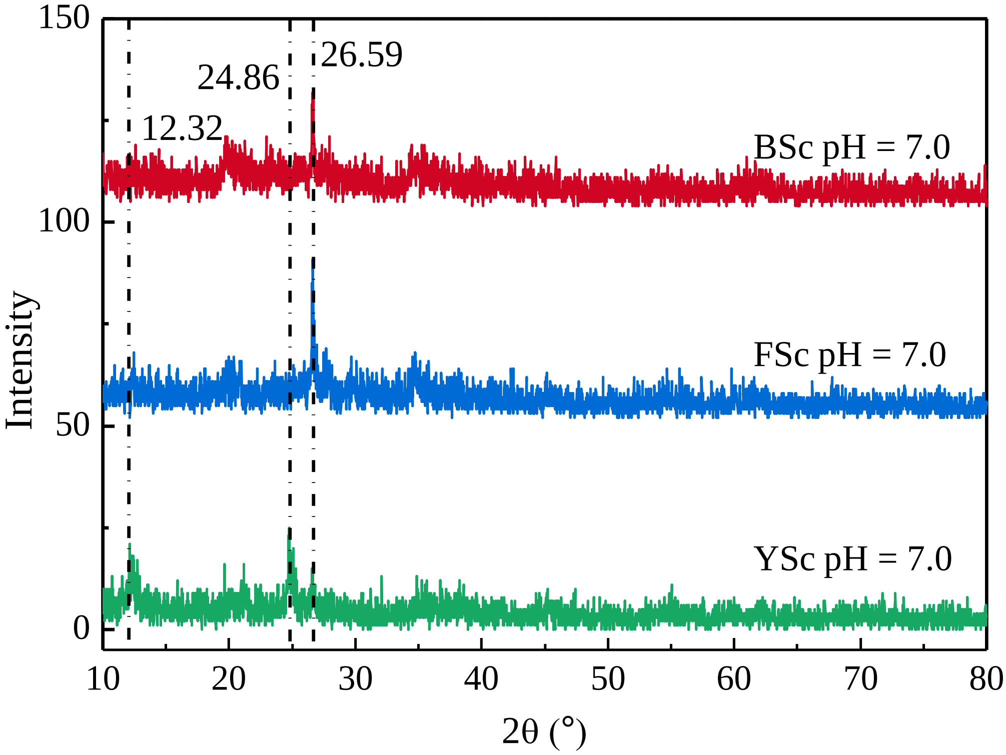

Figure S1. XRD analysis of soil colloids at pH 7.0.

S3. Exponential-model-fitted parameters of settling experiments

Table S1. Exponential-model-fitted parameters of soil colloids and mixed soil colloid-HA/GT at pH 4.0, 7.0, and 9.0.

pH	Colloid	$V_s \times 10^3$ [a] (m h^{-1})	C'_{res} [b] (C_{res}/C_0)	R^2 [c]	Colloid	$V_s \times 10^3$ [a] (m h^{-1})	C'_{res} [b] (C_{res}/C_0)	R^2 [c]	Colloid	$V_s \times 10^3$ [a] (m h^{-1})	C'_{res} [b] (C_{res}/C_0)	R^2 [c]
4		1.20	0.59	0.999		4.02	0.059	0.954		1.01	0.517	0.999
7	BSc	1.05	0.375	0.999	FSc	1.61	0.384	0.997	YSc	1.24	0.432	0.999
9		0.23	-	0.930		0.772	-	0.949		0.364	-	0.995
4		1.79	0.485	0.999		4.0	0.087	0.989		1.75	0.074	0.997
7	BSc-GTc	1.22	0.499	0.999	FSc-GTc	1.29	0.240	0.998	YSc-GT	1.02	0.467	0.998
9		1.17	0.458	0.999		0.762	0.281	0.999		0.788	0.442	0.998
4		0.854	0.471	0.999		1.75	0.532	0.998		0.923	0.453	0.999
7	BSc-HA	0.895	0.491	0.999	FSc-HA	2.22	0.569	0.996	YSc-HA	1.07	0.532	0.999
9		1.11	0.559	0.999		2.08	0.578	0.994		1.12	0.561	0.999

[a] The sedimentation rates; [b] The relative nonsettling concentration; [c] The correlation coefficient for sedimentation model.

S4. Sedimentation kinetics of goethite colloid at different pH

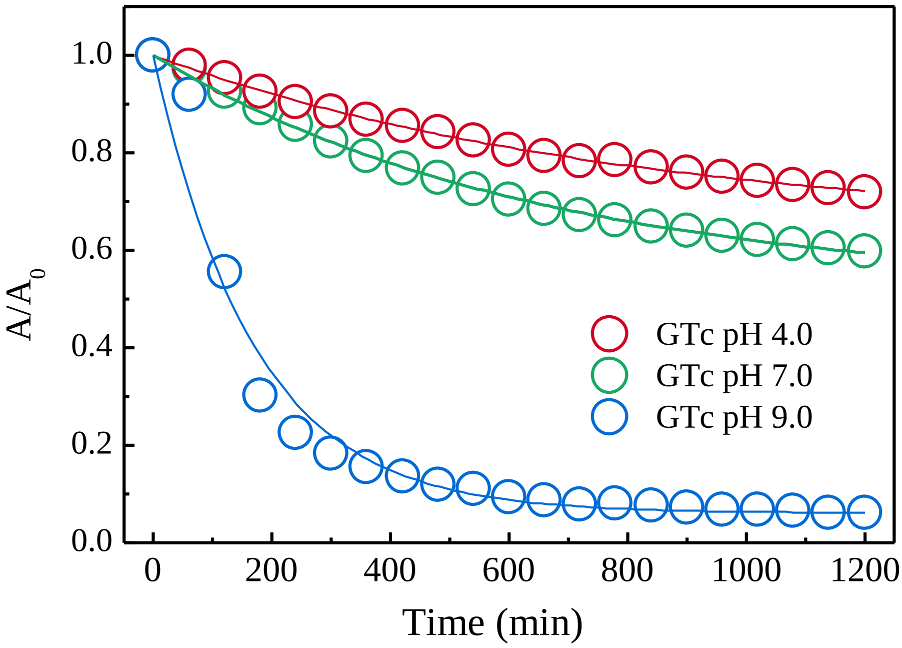

Figure S2. Sedimentation kinetics of goethite (GT) colloid at pH 4.0, 7.0, and 9.0. Symbols show observed data and lines show simulation fitting.

Table S2. Particle size and zeta potential of the goethite (GT) colloid and exponential-model-fitted parameters of goethite (GT) colloid at pH 4.0, 7.0, and 9.0.

pH	Colloid	Particle Size (nm)	Zeta Potential (mV)	$V_s \times 10^3$ [a] (m h^{-1})	C'_{res} [b] ($Cres/C_0$)	R^2 [c]
4		199.5	32.0	1.54	0.519	0.998
7	GTc	382.8	22.1	1.26	0.643	0.998
9		4290.0	7.0	5.94	0.061	0.962

[a] The sedimentation rates; [b] The relative nonsettling concentration; [c] The correlation coefficient for sedimentation model.

S5. Fitted and experimental parameters of transport experiments

Table S3. Fitted and experimental parameters of transport of soil colloids in the sand, 0.5% GT mixed sand, and 0.5% GT–0.2% HA sand columns at pH 7.0.

Column	k_{1a} [a] (min^{-1})	k_{1d} [b] (min^{-1})	k_{2a} [c] (min^{-1})	s_{max2} [d]	k_{1d}/k_{1a}	R^2 [e]	recovery [h] (%)
Q-BS	0.19	0.12	0.02	0.07	0.64	0.99	100.1
Q-GT-BS	0.15	0.09	0.13	0.16	0.60	0.983	93.0
Q-GT-HA-BS	0.18	0.14	0.02	0.12	0.82	0.999	100.5
Q-FS	0.23	0.21	0.00	0.09	0.92	0.999	102.0
Q-GT-FS	0.20	0.17	0.55	1.40	0.83	0.967	68.8
Q-GT-HA-FS	0.17	0.19	0.41	35.57	1.14	0.979	75.8
Q-YS	0.09	0.16	0.00	0.00	1.72	0.990	105.4
Q-GT-YS	0.20	0.08	0.15	0.66	0.41	0.991	87.8
Q-GT-HA-YS	0.19	0.18	0.07	0.55	0.94	0.996	96.6

[a] The first-order retention coefficient on Site-1; [b] The first-order detachment coefficient on Site-1; [c] The first-order retention coefficient on Site-2; [d] Maximum solid phase concentration of nanoparticle on Site-1; [e] Squared Pearson's correlation coefficient; [h] Recovery of soil colloids in the effluent.

water MDPI

S6. The DLVO energy barriers for settling and transport systems

Table S4. The DLVO energy barriers for settling systems.

pH	Colloid	Φ_{MAX} [a] (kt)	Colloid	Φ_{MAX} (kt)	Colloid	Φ_{MAX} (kt)
4		-		-		38.2
7	BS	107.7	FS	-	YS	215.6
9		544.2		-		396.4
4		-		-		-
7	BS-GT	202.4	FS-GT	-	YS-GT	182.3
9		279.2		-		368.6
4		11.8		-		50.2
7	BS-HA	307.6	FS-HA	3.8	YS-HA	388.9
9		366.0		1.8		487.0

[a] The primary energy barriers, its value less than 0 kt express as "-".

Table S5. The primary energy barriers for transport systems.

Column	Φ_{MAX} (kt)
Q-BS	385.7
Q-GT-BS	-
Q-GT-HA-BS	407.2
Q-FS	276.8
Q-GT-FS	-
Q-GT-HA-FS	286.4
Q-YS	753.5
Q-GT-YS	-
Q-GT-HA-YS	829.7

References

1. Bradford, S.A.; Jirka, S.; Mehdi, B.; Martinus, Th. V.G.; Yates, S.R. Modeling colloid attachment, straining, and exclusion in saturated porous media. *Environ. Sci. Technol.* **2003**, *37*, 2242–2250.
2. Yu, B.; Jia, S.Y.; Liu, Y.; Wu, S.H.; Han, X. Mobilization and re-adsorption of arsenate on ferrihydrite and hematite in the presence of oxalate. *J. Hazard. Mater*. **2013**, *262*: 701–708.